Wavelength selective filter based on polarization control in a photonic bandgap structure with a defect

Ana Andres-Arroyo,[1] Peter J. Reece,[1,*] Craig M. Johnson,[1] Kaushal Vora,[2] Fouad Karouta,[2] and Chennupati Jagadish[2]

[1]*School of Physics, The University of New South Wales, Sydney, NSW 2052, Australia*
[2]*Research School of Physics and Engineering, The Australian National University, Canberra, ACT 0200, Australia*

[*]*p.reece@unsw.edu.au*

Abstract: We present a technique for achieving wavelength specific half-wave retardation upon reflection from an asymmetric one-dimensional photonic band-gap structure with a defect. The approach is based on a high finesse Gires-Tournois type interferometer and makes use of the large mode splitting of TE and TM defect modes that occurs in structures with a wide photonic band-gap. We use this structure to demonstrate a polarization-based selective tuneable filter with a narrow pass-band and wide rejection-band.

© 2011 Optical Society of America

OCIS codes: (310.0310) Thin films; (230.7408) Wavelength filtering devices; (230.5440) Polarization-selective devices.

References and links

1. L. Wu, M. Mazilu, J.-F. Gallet, T. F. Krauss, A. Jugessur, and R. M. D. L. Rue, "Planar photonic crystal polarization splitter," Opt. Lett. **29**(14), 1620–1622 (2004). URL http://ol.osa.org/abstract.cfm?URI=ol-29-14-1620.
2. D. M. Beggs, T. P. White, L. O'Faolain, and T. F. Krauss, "Ultracompact and low-power optical switch based on silicon photonic crystals," Opt. Lett. **33**(2), 147–149 (2008). URL http://ol.osa.org/abstract.cfm?URI=ol-33-2-147.
3. P. Yeh, *Optical Waves in Layered Media*, Wiley Series in Pure and Applied Optics (Wiley-Interscience, 2005). ISBN: 978-0-471-73192-4.
4. F. Gires and P. Tournois, "An Interferometer useful for pulse compression of a frequency-modulated light pulse," C. R. Acad. Sci. (Paris) **258**, 6112 (1964).
5. Q. F. Dai, Y. W. Li, and H. Z. Wang, "Broadband two-dimensional photonic crystal wave plate," Appl. Phys. Lett. **89**(6), 061121 (2006). URL http://dx.doi.org/doi/10.1063/1.2243798.
6. K. Wu, J. Dong, and H. Wang, "Phase engineering of one-dimensional defective photonic crystal and applications," Appl. Phys. B: Lasers Opt. **91**, 145–148 (2008). URL http://dx.doi.org/10.1007/s00340-008-2957-y.
7. J. J. Saarinen, S. M. Weiss, P. M. Fauchet, and J. E. Sipe, "Reflectance analysis of a multilayer one-dimensional porous silicon structure: Theory and experiment," J. Appl. Phys. **104**(1), 013103 (2008). URL http://dx.doi.org/doi/10.1063/1.2949265.
8. R. P. Stanley, R. Houdré, U. Oesterle, M. Gailhanou, and M. Ilegems, "Ultrahigh finesse microcavity with distributed Bragg reflectors," Appl. Phys. Lett. **65**(15), 1883–1885 (1994). URL http://dx.doi.org/doi/10.1063/1.112877.
9. O. Y., "A new monochromator," Nature **41**, 157–158 (1938). URL http://dx.doi.org/10.1038/141157a0.
10. I. ŠOLC, "Birefringent Chain Filters," J. Opt. Soc. Am. **55**(6), 621–625 (1965). URL http://www.opticsinfobase.org/abstract.cfm?URI=josa-55-6-621.

1. Introduction

Photonic band-gap engineering is an established technique for creating optical functionality through structuring of materials on the wavelength scale. By periodically modulating refractive index, the optical properties of materials can be tuned from transparent to highly reflective over specified spectral bands. Waveguide technology based on two-dimensional photonic crystals provides compact integrated optical circuits with a wide range of functional devices. In addition to reflection and transmission, polarization and phase of light may be manipulated in periodically modulated media for devices such as polarizing beam splitters [1] and interferometric-based optical switches [2].

In the case of one-dimensional photonic structures there are also possibilities to control the phase and polarization of light. Early examples of phase-based optical elements include the Gires-Tournois interferometer; a low finesse asymmetric optical resonator with a highly reflective back mirror (100% reflectivity) [3]. This type of device, used for generating chromatic dispersion in ultra-fast pulse shaping, makes use of the 2π phase change that occurs at the cavity resonant wavelength [4].

Recently it was suggested by Dai *et al.* that rich polarization dependent phase structuring present in the pass-band of a one-dimensional photonic crystal may be used to fabricate wave plates [5]. However, the strong angular dependent modulation of the amplitude of the reflected and transmitted waves in these bands severely limits practicability in terms of optical elements. The same group presented a theoretical approach to using multiple defects within the stop band of a photonic crystal to overcome the effects of changes in the intensity of the reflected light [6].

In this report we exploit the large splitting between TE and TM defect modes present in wide band-gap photonic structures to demonstrate a wavelength selective half-wave plate for light reflected at non-normal incidence. Placed between two crossed polarizing beam splitters, light in a tuneable narrow spectral band may be filtered from a broad spectrum. This structure is realised experimentally using a deposited multilayered structure consisting of silicon oxide (SiO_x) and amorphous silicon (a-Si) with optical parameters designed for the telecommunications band around 1550 nm.

2. Design and Fabrication

SiO_x/a-Si multi-layered structures are prepared using plasma enhanced chemical vapour deposition (PECVD) (Oxford Instruments). Prior to deposition the Si substrate is cleaned in HF (10%), rinsed and blown-dry in N_2. All layers are grown in one run at 300°C using: SiH_4:N_2O:N_2 (9:710:160 sccm), at a pressure of 650 mTorr and an RF power of 20W for the SiO_x layers; and SiH_4:He (25:475 sccm), at a pressure of 1 Torr and an RF power of 10W for the a-Si layers. These materials are chosen to achieve a very large refractive index contrast within the structure and minimum absorption losses in the near infrared beyond the absorption edge of a-Si. As a-Si is transparent down to the near IR/red spectrum, this material combination is suitable as high reflectivity coatings in GaAs-based laser application. A schematic diagram of the photonic structure is depicted in Fig. 1(insert). The structure consists of a twelve-period Bragg reflector with a low refractive index defect layer inserted after three periods.

A simulated reflectance spectrum of this structure, for light incidence at 35°, is shown in Fig. 1(a); both TE and TM polarization states are included. The reflectivity is calculated using the Transfer Matrix Method and includes material dispersion and absorption for both a-Si and SiO_x layers. The large refractive index difference between the alternating layers produces a broad high reflectivity spectral band in the near infrared. No optical resonance is observed in reflectivity spectrum due to the inclusion of the cavity layer. This is because the asymmetric structure design allows only light to be coupled to the cavity layer via the top mirror.

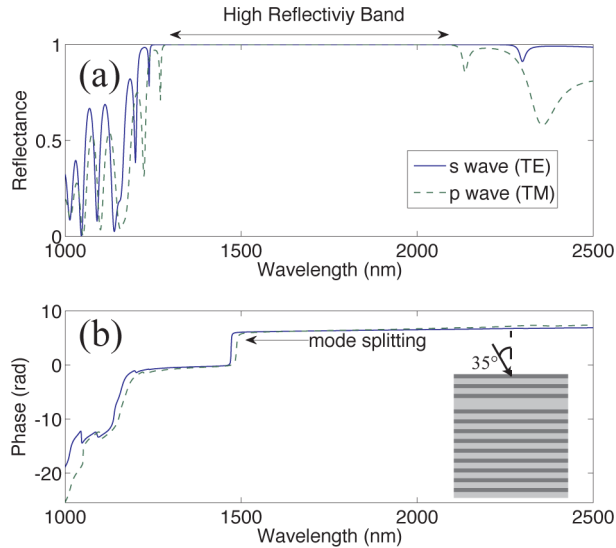When considering the phase of light reflected from this structure, shown in Fig. 1(b), it

Fig. 1. (a) Simulated reflectivity spectrum of an asymmetric photonic crystal with a defect with light incident at 35° for TE and TM polarizations. (b) Corresponding phase change upon reflection from this structure. At the resonance wavelength there is a 2π phase change occurs; for wide photonic band-gap structures polarization dependent mode splitting is observed. (insert) Structure consists of alternate layers of PECVD deposited SiO_x and a-Si in a twelve-period Bragg reflector with a low refractive index defect layer inserted after three periods.

is noted that a 2π phase change occurs at the position of the optical resonance; this feature persists even in the absence of an observable resonance dip in reflectivity. We also note that when light is incident on the structure at non-normal incidence, the resonance for TE and TM polarization states occurs at different spectral positions. The mode splitting is due to differences in phase changes for the different polarization states upon reflection from the periodic layers. At normal incidence the TE and TM mode are identical, but as the reflection of the TM wave from each layer boundary is reduced at non-normal incidence, the mode penetrates deeper in the photonic structure and the effective cavity length is increased [7]. The effect is most pronounced in half wavelength defect layers where the penetration length in the photonic crystal is significant compared to the cavity layer [8]. For photonic structures with very small refractive index modulation the mode splitting it very small, typically less than the line width of the resonance.

Figure 2(a) depicts an optical arrangement which utilises the resonance mode splitting and the 2π phase change to selectively filter a narrow wavelength band. In this arrangement a polarizing beam splitter (PBS) is used to set the light incident on the photonic crystal with polarization set to 45° with respect to the plane of incidence, thereby providing equal amounts of TE and TM polarization. The polarized light is reflected off the structure at incident angle, θ and passed through a second PBS in an orthogonal configuration.

Figure 2(b) shows details of the phase upon reflection from the photonic structure for each of the polarization states and the resulting transmission though the crossed-polarizer. Note that the transmission is normalised to the light field after the first polarizer. Importantly, at the resonant wavelengths, marked as (2) and (4) in the diagram, there will be π phase shift between the two polarization states, and the effective polarization state of the reflected light will be rotated by 90°. Figure 2(c) shows a graphical representation of the polarization orientation at
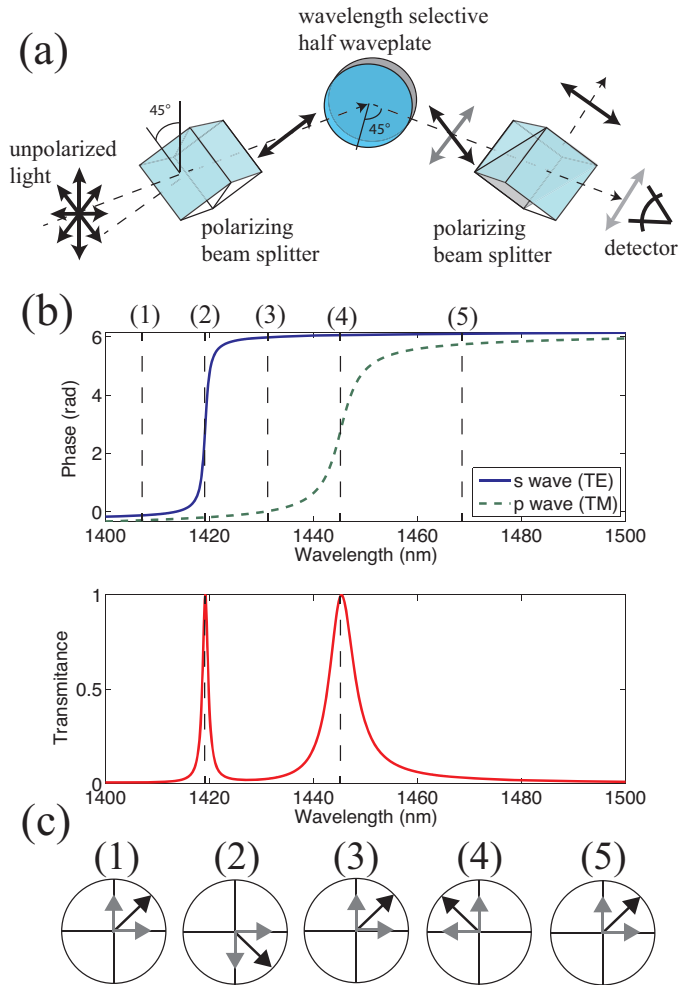
Fig. 2. (a) Optical arrangement used to demonstrate wavelength selective filtering based on the wide photonic band-gap structure described in Fig. 1. The top graph in (b) shows the relative phase change versus wavelength around the optical resonance for light incident at 45° for both TE and TM polarization states and whilst the bottom graph shows the corresponding transmission through the optical arrangement described in 2(a). Graph (c) shows the schematic representation of the polarization orientation for the TE wave, TM wave and resultant polarization at different points in the spectrum.

selected spectral positions around the resonance. The combination of the two polarizers and the wavelength selective half-wave plate leads to the selection of two narrow spectral bands. The rejection band of such an arrangement is determined by the width of the high reflectivity band, and can be several hundred nanometers for structures which have large refractive index differences in the mirrors. The overall width of the transmission bands are determined by the number of periods in the structure before the defect layer and the full width half maximum for the TE polarization case is always sharper because the stronger reflection from periodic layers leads to a higher finesse resonance.
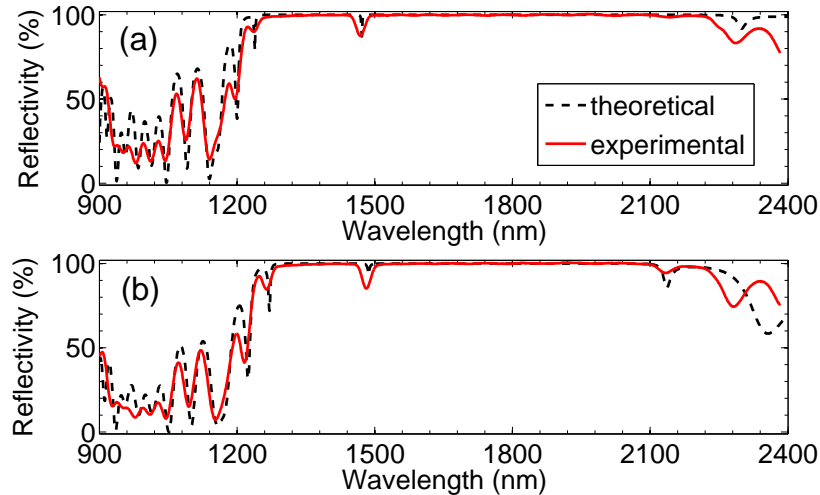
Fig. 3. Measured and simulated reflectance of the (a) TE (s-) polarization (b) and the TM (p-) polarization states for an incident angle of 35°. The reflectivity dip is located at 1468 nm for TE polarization and 1487 nm for TM polarization. The presence of a dip in the measured reflectivity indicates that there are scattering losses within the films. The structure consists of alternate layers of SiO_x and a-Si in a twelve-period Bragg reflector with a low refractive index defect layer inserted after three periods. The simulated parameters were 135 nm and 248 nm for a-Si and SiO_x layers respectively. The corresponding refractive index values (at 1550 nm) were estimated to be 3.688 and 1.467.

3. Experimental Results

Figure 3 shows the experimentally measured and simulated reflectivity spectrum of the a-Si/SiO_x multilayer at an incident angle of 35° for both TE (a) and TM (b) polarization states. The reflectivity dip is located at 1468 nm for TE polarisation and 1487 nm for TM polarization. Reflectivity measurements were made using a PerkinElmer Lambda 1050 Spectrophotometer. The layer thicknesses used for the simulation were 135 nm and 248 nm for a-Si and SiO_x layers respectively. The corresponding refractive index values (at 1550 nm) were estimated to be 3.688 and 1.467. The simulation shows excellent agreement for both polarization states over the spectral region of interest. We note that there are small but observable dips in the reflectance spectra at the resonance position that we attribute to the presence of scattering losses at the dielectric interfaces. The magnitude of the dips may be accounted for by introducing an effective loss coefficient of 25.0 cm^{-1} into the simulation. Cross-sectional scanning electron microscope (SEM) images, presented in Fig. 4, also provides evidence for non-negligible roughness at the dielectric interface with typical amplitude of the order of 10 nm (see insert). Physical thicknesses for the layers are estimated to be 143 nm and 243 nm, and are in close agreements with those determined by optical simulation. We note that the thicknesses are deliberately chosen not to correspond to quarter wave thicknesses in the photonic structure, but to maximise the mode splitting at non-normal incidence.

Optical measurements following the arrangements presented in Fig. 2(a) were used to test the optical response of the wavelength selective half-wave plate. In these experiments a fiber-coupled incoherent white light source (Mikropack) is collimated in free-space and passed through a broadband polarizing beam splitter (CVI Optics). The polarized light is focused onto the sample using a 15 cm focal length lens at a selected angle of incidence and the reflected
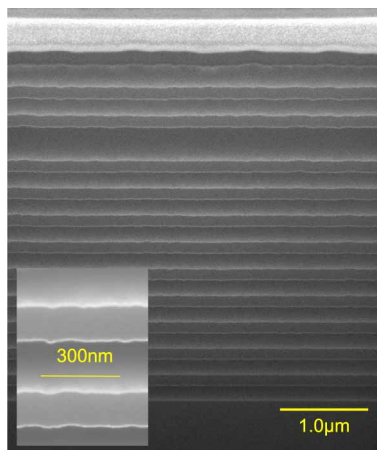
Fig. 4. Cross-sectional scanning electron micrograph image of the photonic structure. Insert: higher magnification (3x) image showing details of the a-Si/SiO$_x$ interface. Structure consists of alternate layers of PECVD deposited SiO$_x$ and a-Si in a twelve-period Bragg reflector with a low refractive index defect layer inserted after three periods. Sample cross-sections were prepared by focused ion beam milling (FEI Helios).

light is passed through a crossed polarizer, coupled into an optical fiber, and analysed using a compact NIR spectrometer (Ocean Optics NIR512).

In Fig. 5(a), a simulation is presented of the transmission through the second polarizer upon reflection from the photonic structure in the spectral region around the stop band for incident angles between 0° and 70°. In this two-dimensional plot white indicates minimum transmission and black is maximum. It is clear that at small angles of incidence the transmission is low everywhere as the phase change upon reflection is equal for both polarization states. Above an angle of 10° the splitting becomes significant and the transmission at the resonance wavelength increases. Above 20° two resonance peaks are observed and maximum transmission is observed. We also observe low levels of transmission outside the stop band. Further mode splitting occurs at larger angles and the modes shift to shorter wavelengths. The overall reduction in the rejection band at larger angles of incidence is due to the diminishing size of the stop-band of the TE polarization state at large angles of incidence.

Figures 5(b)–(d) shows the transmission spectrum of light incident on the wavelength selective half-wave plate at 25°, 35° and 45° with the corresponding simulations. We note excellent qualitative agreement between the experimental and simulated results, including the shape and position of complex spectral features in the transmission band and on resonance. At 25° the transmission within the stop-band is less than 0.1%, whilst the pass-band had a FWHM of 12 nm; in this instance the two modes are not fully resolved. At larger angles of incidence the transmission band exhibits the expected double peak shape, which is fully resolved at 45°. The widths of the peaks are in agreement with the simulation and are limited by the low number of periods of the photonic structure before the defect mode. The peak transmission at the resonance wavelength is approximately 50% which is lower than the expected 100% from the simulation. We associate this with the introduction of scattering due to surface roughness at the dielectric interfaces. This is the primary limitation for moving to higher finesse structures using this material system.

Experimentally measured peak positions for each of the different angles of incidence are also in good agreement with simulation. The simulated values match most precisely with ex-
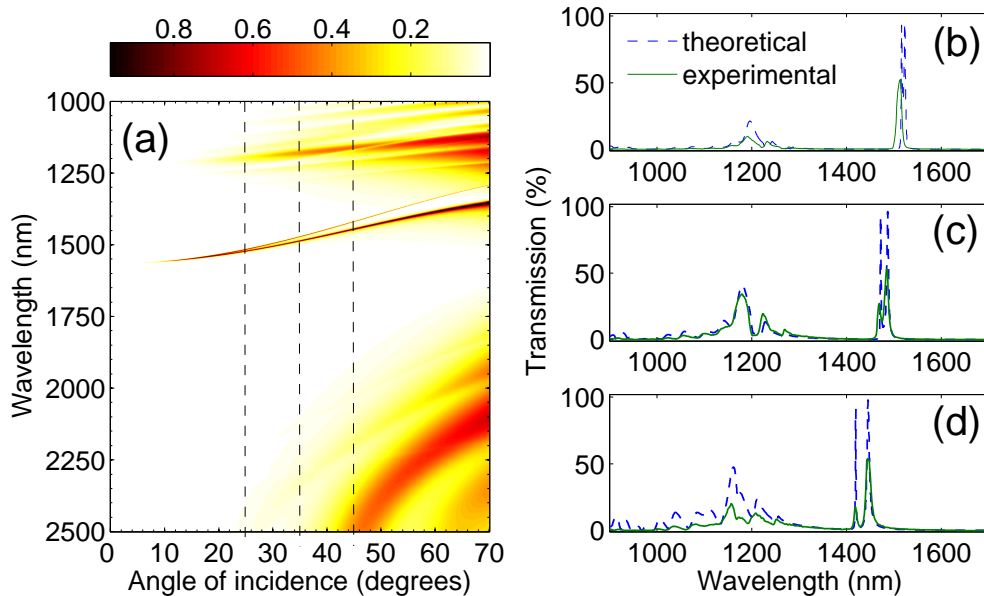
Fig. 5. (a) 2D plot of the transmission through crossed polarizers for angles of incidence between 0° and 70°. We see that for small angles of incidence, no mode splitting is observed and the transmission through the polarizers is very low. Appreciable mode splitting, and hence transmission, is observed above 25. Experimentally measured (solid) and simulated (dotted) transmission spectra through crossed polarizers with incident angles of 25° (b), 35° (c) and 45° (d). The corresponding experimentally determined peak positions for each angle of incidence are (b) 1513nm at 25°, (c) 1469 nm and 1484 nm at 35°, and (d) 1419 nm and 1446 nm at 45°.

periment at an incidence of 45°, where the peak positions were at 1419 nm and 1446 nm. At an incidence of 35° the measured peak transmission were measured at 1469 nm and 1484 nm and the simulated values correspond to 1472 nm and 1487 nm. At an incidence of 25° a single peak is resolved at 1513nm where as the simulated values predict a double humped peak at 1516 nm and 1523 nm. The small discrepancy in the peak positions is largely due to imprecise determination of the refractive index dispersion of the deposited materials.

This method for achieving wavelength selective filtering has a number of distinguishing properties: strong wavelength suppression over a large spectral region is achieved using the crossed polarizers and can have an extinction ratio of up to 10^6; a wide rejection band extending several hundred nanometers results from the large refractive index modulation present in the photonic structure; and the FWHM is achieved by the sharp phase change upon reflection at the defect resonance. If two of these interferometer arrangements are used in parallel then, in principle, 100% transmission from unpolarized light may be achieved; two arrangements in series may be used to produce a single peaked transmission. This is in comparison with other phase-based spectral filters that employ conventional wave plates, such as the Lyot - Ohman [9] and Sloc filters [10], which require a large number of components in series to achieve the desired filtering. Further if the deflected component of light from the second PBS is utilised the filter design can be used as an add-drop multiplexer for optical networks or an notch / edge filter for Raman spectroscopy. The optical filter arrangement described has limitations similar to other interference based filters in term of high numerical aperture (NA) operation. The effect of the

NA on the transmission of the can be inferred from the dispersion of the resonant modes shown in Fig. 5(a). Incident light that covers a broad range of incident angles on the wave plate will experience an averaging effect, thereby reducing the peak transmission and broadening the peak width.

With further refinement of the fabrication process to improve the scattering losses of the films filters with sharper resonances and a higher peak transmission are possible. Chirping of the Bragg mirrors may be used to increase the spectral range of the high reflectivity band, which will increase the rejection band of the filter. Chirping may also be used to increase the separation between the TE and TM modes and fine-tune the finesse of the individual resonances. The incorporation of different defect layer thicknesses can be used to control the position of the resonance with respect to the band edge.

4. Conclusion

In conclusion, we have demonstrated a technique for achieving wavelength specific half-wave retardation upon reflection from an asymmetric wide photonic band-gap structure with a defect. In combination with crossed-polarizers, we demonstrate tuneable narrow-band spectral filter where the transmission properties are determined by the polarization state of the reflected light. We have experimentally realised this device in the telecommunications band using a deposited multilayered structure consisting of silicon oxide (SiO_x) and amorphous silicon (a-Si).

Acknowledgments